

Efficient collection of excitation energy from a linear-shaped weakly interacted perylenetetracarboxylic diimides array†

Cite this: *Phys. Chem. Chem. Phys.*, 2013, **15**, 17342

Guiju Qi,^a Lilin Jiang,^b Yingyuan Zhao,^a Yanqiang Yang^{*b} and Xiyou Li^{*a}

A series of novel light-harvesting compounds (namely PO–PN, PO–PO–PN and PO–PO–PO–PN) were synthesized with a linear-shaped phenoxy group-substituted perylenetetracarboxylic diimide (PO) oligomer as donor and a pyrrolidinyll group-substituted perylenetetracarboxylic diimide (PN) as acceptor. The photophysical properties of these linear-shaped compounds are investigated by steady state electronic absorption, fluorescence spectra and lifetime measurements. The ground state interactions between the neighbor PO subunits within these three compounds are weak. No matter which PO subunit is excited in these linear molecules, the excitation energy is finally collected by the PN subunit. The excitation energy can transfer as long as 47 Å without any decrease in efficiency. The energy transfer rate constants determined by femto-second transient absorption experiments are fast and close to that of the energy transfer from B800 to B850 in LH II of natural photosynthesis.

Received 14th July 2013,
Accepted 22nd August 2013

DOI: 10.1039/c3cp52941j

www.rsc.org/pccp

Introduction

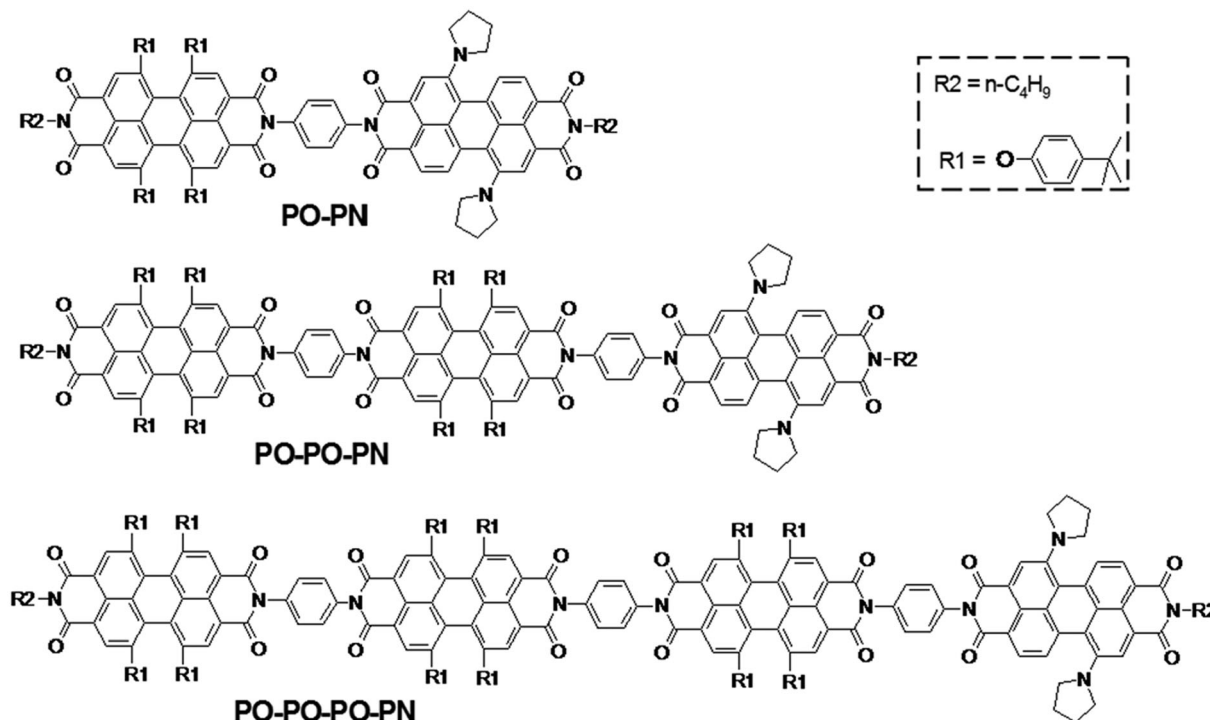
To match the ever-growing demand for renewable and sustainable energy sources, scientists with different disciplines of chemistry try to duplicate the photoinduced processes in the light-harvesting systems of natural photosynthesis in simple chemical systems.^{1–5} The systems composed of multiple chromophores are particularly important,^{6–11} because the light-harvesting system of natural photosynthesis contains tens of chlorophyll molecules, which are organized by supramolecular interactions in an ordered structure. The most popularly investigated organic dyes in this field are porphyrins because of their similar molecular structure and photophysical properties with natural bacteriochlorophyll *a* (Bchl *a*) molecules.^{12–25} Porphyrin arrays with linear structure or cyclic structure are constructed and the photophysical properties are investigated. Most of these researches are focused on the excitation migration between porphyrin subunits within these molecular arrays. A communication which reported an energy transfer between two different cyclic porphyrin arrays in a thin film represents new progress in this field.²⁶

Besides porphyrin arrays, perylenetetracarboxylic diimide (PDI) dyes have also attracted a great deal of attention in the past decade due to their exceptional chemical and thermal stabilities in combination with high extinction coefficients.^{27–34} Similar to porphyrin arrays, PDI arrays with ordered structures connected by covalent bonds or supramolecular interactions are constructed and the photophysical properties are investigated. One group of PDI arrays with well defined structure is designed and prepared for the purpose of revealing the structure–property relationship for a PDI array, such as the face-to-face stacked dimers^{35,36} and trimers^{37,38} which show blue-shifted absorption band and excimer-like emission. The photophysical properties of these PDI arrays can be explained as the result of the interactions between two parallel arranged transition dipole moments following exciton theory. Branched PDI hexamer,³⁹ trimer,⁴⁰ and dendron-like PDI compounds were also previously achieved by using a rigid backbone.^{41–48} The system relates to a synthetic linear rigid trichromophoric perylenediimide (3PDI) that was studied by Hooenboom *et al.* and Hernando *et al.*^{49–52} A strong interaction and bathochromic shift was observed and exciton delocalization was revealed by the reduced fluorescence lifetimes. In another rigid and linear structure existing of three PDI chromophores linked together by diphenyl-acetylene units (3PDIAC),⁵³ weak interactions between the neighbour PDIs were found and it behaves as a single emitter. Another group of PDI arrays was designed for the purpose of achieving efficient energy transfer among the molecular arrays. A cascade energy transfer was found between the PDI subunits with different side groups at bay positions in the gel system.⁵⁴ Similar energy

^a Key Laboratory of Colloid and Interface Chemistry, Department of Chemistry, Shandong University, Shanda nan lu 27#, Jinan, 250100, China.
E-mail: xiyouli@sdu.edu.cn; Fax: +86-531-88564464

^b Center for Condensed Matter Science and Technology, Department of Physics, Harbin Institute of Technology, Harbin 150001, China. E-mail: yqyang@hit.edu.cn

† Electronic supplementary information (ESI) available: Additional spectroscopic data, calculation of energy transfer parameters following the Förster theory, transient absorption spectra of PO–PN, PO–PO–PN, and PO–PO–PO–PN, decay profiles of PO–PO–PO–PN and the fitting results. See DOI: 10.1039/c3cp52941j



Scheme 1 Molecular structures of the title compounds.

transfer was reported by Würthner in a calixarene-based cofacially-positioned PDI array.⁵⁵ A pancake-like molecule, which is composed of four PDI subunits and a central phthalocyanine unit, can stack in a face-to-face way to form molecular aggregates.⁵⁶ Efficient and quick energy transfer from the PDI aggregates to phthalocyanine aggregates was found in this system. Up to now, the interactions between/among the PDI units with precisely controlled relative orientations have been extensively studied. But the collection of excited energy from these energy donors with precisely controlled structures is scarcely reported in the literature. How the interactions between the donors affect the energy transfer to an acceptor is still an open question, not only for the PDI systems, but also for other multiple chromophore systems, such as porphyrin systems. Model compounds composed of not only multiple PDI donors with precisely controlled relative interactions but also a proper acceptor are needed to answer this question.

In this contribution, we have synthesized a series of rigid linear PDI-based donor-acceptor oligomers linked together by a phenyl bridge, namely, PO-PN, PO-PO-PN and PO-PO-PO-PN, as shown in Scheme 1. Here PO represents a PDI derivative with two *tert*-butylphenoxy groups at the 1 and 7 positions, while PN represents a PDI derivative with two pyrrolidinyl groups at the 1 and 7 positions. The emission of the PO unit overlaps very well with the absorption of the PN unit, therefore, excitation energy can be transferred from PO to PN. This has been well documented in the literature.⁵⁷ More importantly, Förster type energy hopping between neighbour POs is possible in these three compounds.⁵³ The most important characteristic of these molecules is the relative weak ground interactions between the neighbour PO subunits, which can keep the excitation energy hopping between

neighbour PDI subunits, and meanwhile, can reduce the non-radiative decay for the excited states in the PO array. The latter may be helpful to achieve a long distance energy transfer without an obvious efficiency decrease. To the best of our knowledge, this represents the first example of the experimental study on energy transfer from a weakly coupled linear donor array to an acceptor.

Experimental

General methods

¹H NMR spectra were recorded at 300 MHz with the solvent peak as internal standard (in CDCl₃). Electronic absorption spectra were recorded on a Hitachi 4100 spectrometer. Fluorescence spectra were measured on an ISS K2 system while the fluorescence quantum yields were calculated with *N,N'*-dicyclohexylperylene-3,4:9,10-tetracarboxylic diimide ($\Phi_f = 100\%$) as standard. MALDI-TOF mass spectra were obtained on a Bruker BIFLEX III mass spectrometer with α -cyano-4-hydroxycinnamic acid as matrix. The femtosecond time-resolved spectrometer employs a regenerative Ti:sapphire amplifier (Spitfire, Spectra Physics) as the primary beam source. The output pulse (120 fs, 1 kHz, 800 nm) was split into two beams by a beam splitter (90 and 10%). The 90% beam pumped an optical parametric amplifier (OPA-800FC, Spectra Physics) to produce the pump pulse with a centered wavelength of 530 nm. The other one was focused by a lens on the water to produce the white light supercontinuum. The white light supercontinuum was split into two equal beams, which were respectively used as the probe and reference beams. The polarization of the pump pulse

was paralleled with that of the probe pulse. In order to avoid destruction of the sample, the cuvette with path length 1 mm was mounted on a translation stage with the appropriate speed.

Materials

N,N'-Dicyclohexyl-1,7-di(pyrrolidinyl)perylene-3,4:9,10-tetracarboxylic diimide (**1**),⁵⁸ and *N,N'*-dicyclohexyl-1,6,7,12-tetra(4-*t*-butylphenoxy)perylene-3,4:9,10-tetracarboxylic diimide (**2**)⁵⁹ were prepared following the literature methods. 1,6,7,12-Tetra(4-*t*-butylphenoxy)perylene-3,4:9,10-tetracarboxylic dianhydride and 1,7-di(pyrrolidinyl)perylene-3,4:9,10-tetracarboxylic dianhydride were prepared by the hydrolysis of corresponding diimide compounds in *n*-propanol with potassium hydroxide following the published procedures.⁶⁰ *N-n*-Butyl-1,6,7,12-tetra(4-*t*-butylphenoxy)perylene-3,4:9,10-tetracarboxylic-3,4-anhydride-9,10-imide (**3**)⁶¹ and *N-n*-butyl-1,7-di(pyrrolidinyl)perylene-3,4:9,10-tetracarboxylic-3,4-anhydride-9,10-imide (**4**)⁶² were prepared according to the literature. The compounds above were fully characterized by ¹H NMR and MALDI-TOF mass spectra. All other chemicals are purchased from commercial sources and used as received without further purification.

***N-n*-Butyl-*N-p*-phenylenediamine-1,6,7,12-tetra(4-*t*-butylphenoxy)perylene-3,4:9,10-tetracarboxylic diimide (**5**)**. *N-n*-Butyl-1,6,7,12-tetra(4-*t*-butylphenoxy)perylene-3,4:9,10-tetracarboxylic-3,4-anhydride-9,10-imide (**3**) (156 mg, 0.15 mmol) and *p*-phenylenediamine (20 mg, 0.18 mmol) in 50 ml of pyridine were refluxed for 36 h. After the solvent was evaporated under reduced pressure, the residue was purified by column chromatography on silica gel using CHCl₃-MeOH (1000:1, v/v) as eluent. After recrystallization from chloroform and methanol, the product was collected as purple solid (130 mg, 79%). Mp. > 300 °C; ¹H NMR (300 MHz, CDCl₃, TMS): 8.27 (s, 2H), 8.21 (s, 2H), 7.36 (s, 4H), 7.24 (m, 8H), 6.82 (m, 8H), 4.11 (t, 2H), 1.65 (m, 2H), 1.37 (m, 2H), 1.29 (s, 36H), 0.93 (t, 3H). MS(MALDI-TOF): *m/z*, calculated for C₇₄H₇₁N₃O₈: 1130.37, found 1130.31 [M⁺]. Elemental analysis (%), calculated for C₇₄H₇₁N₃O₈: C 78.63, H 6.33, N 3.72; found: C 78.61, H 6.29, N 3.75.

Compound 6. A mixture of *N-n*-butyl-*N-p*-phenylenediamine-1,6,7,12-tetra(4-*t*-butylphenoxy)perylene-3,4:9,10-tetracarboxylic diimide (**5**) (150 mg, 0.13 mmol), imidazole (1.5 g), and 1,6,7,12-tetra(4-*t*-butylphenoxy)perylene-3,4:9,10-tetracarboxylic acid anhydride (**2**) (260 mg, 0.26 mmol) in toluene (15 ml) was heated to reflux and kept at reflux for 48 h. The solvents were then removed under reduced pressure and the residue was washed with water. The product was purified by column chromatography on silica gel with chloroform-petroleum ether (10:11, v/v) as eluent. After recrystallization from chloroform and methanol, the product was collected as a red solid (45 mg, 30%). Mp. > 300 °C; ¹H NMR (300 MHz, CDCl₃, TMS): 8.22 (m, 8H), 7.36 (s, 4H), 7.23 (m, 16H), 6.83 (m, 16H), 4.11 (t, 2H), 1.64 (m, 2H), 1.40 (m, 2H), 1.28 (m, 72H), 0.93 (t, 3H). MS (MALDI-TOF): *m/z*, calculated for C₁₃₈H₁₂₅N₃O₁₇: 2097.48, found 2098.01 [M⁺]. Elemental analysis (%), calculated for C₁₃₈H₁₂₅N₃O₁₇: C 79.02, H 6.01, N 2.00; found: C 79.04, H 5.98, N 1.95.

Compound 7. Compound **6** (104 mg, 0.05 mmol) and *p*-phenylenediamine (6.5 mg, 0.06 mmol) in 50 ml of pyridine were refluxed for 24 h. After the solvent was evaporated under reduced pressure, the residue was purified by column chromatography on silica gel using CHCl₃-MeOH (1000:1, v/v) as the eluent. After recrystallization from chloroform and methanol, the product was collected as purple solid (45.8 mg, 42%). Mp. > 300 °C; ¹H NMR (300 MHz, CDCl₃, TMS): 8.24 (m, 8H), 7.38 (s, 4H), 7.21 (m, 16H), 7.0 (br, 2H), 6.83 (m, 16H), 4.11 (t, 2H), 1.65 (m, 2H), 1.28 (m, 2H), 1.25 (m, 72H), 0.91 (t, 3H). MS (MALDI-TOF): *m/z*, calculated for C₁₄₄H₁₃₁N₅O₁₆: 2187.6, found 2187.13 [M⁺]. Elemental analysis (%), calculated for C₁₄₄H₁₃₁N₅O₁₆: C 79.06, H 6.04, N 3.02; found: C 79.04, H 6.10, N 2.96.

Compound 8. A mixture of **7** (44 mg, 0.02 mmol), imidazole (500 mg), and 1,6,7,12-tetra(4-*t*-butylphenoxy)perylene-3,4:9,10-tetracarboxylic acid anhydride (**2**) (40 mg, 0.04 mmol) in toluene (25 ml) was heated to reflux and kept at reflux for 48 h. The solvents were removed under reduced pressure and the residue was washed with water. The product was purified by column chromatography on silica gel with chloroform-methanol (1000:1, v/v) as eluent. After recrystallization from chloroform and methanol, compound **8** was collected as a red solid (12 mg, 20%). Mp. > 300 °C; ¹H NMR (300 MHz, CDCl₃, TMS): 8.24 (m, 12H), 7.37 (s, 8H), 7.20 (m, 24H), 6.84 (m, 24H), 4.11 (t, 2H), 1.64 (m, 2H), 1.28 (m, 2H), 1.25 (m, 108H), 0.85 (t, 3H). MS (MALDI-TOF): *m/z*, calculated for C₂₀₈H₁₈₅N₅O₂₅: 3154.71, found 3154.82 [M⁺]. Elemental analysis (%), calculated for C₂₀₈H₁₈₅N₅O₂₅: C 79.19, H 5.91, N 2.22; found: C 79.14, H 5.90, N 2.25.

***N-n*-Butyl-*N-p*-phenylenediamine-1,7-di(pyrrolidinyl)perylene-3,4:9,10-tetracarboxylic diimide (**9**)**. *N-n*-Butyl-1,7-di(pyrrolidinyl)perylene-3,4:9,10-tetracarboxylic-3,4-anhydride-9,10-imide (**4**) (50 mg, 0.08 mmol) and *p*-phenylenediamine (11 mg, 0.1 mmol) in 25 ml of pyridine were refluxed for 24 h. After the solvent was evaporated under reduced pressure, the residue was purified by column chromatography on silica gel using CHCl₃-MeOH (1000:5, v/v) as the eluent. After recrystallization from chloroform and methanol, the product was collected as purple solid (14 mg, 25%). Mp. > 300 °C; ¹H NMR (300 MHz, CDCl₃, TMS): 8.45 (m, 4H), 7.68 (s, 2H), 7.13 (d, 2H), 6.83 (m, 2H), 4.23 (t, 2H), 3.74 (br, 4H), 2.83 (br, 4H), 2.06 (br, 8H), 1.77 (m, 2H), 1.48 (m, 2H), 0.98 (t, 3H). MS (MALDI-TOF): *m/z*, calculated for C₄₂H₃₇N₅O₄: 675.77, found 676.29 [M⁺]. Elemental analysis (%), calculated for C₄₂H₃₇N₅O₄: C 74.43, H 5.50, N 8.27; found: C 74.44, H 5.48, N 8.24.

PO-PO. The mixture of *N-n*-butyl-1,6,7,12-tetra(4-*t*-butylphenoxy)perylene-3,4:9,10-tetra carboxylic-3,4-anhydride-9,10-imide (100 mg, 0.09 mmol) and *p*-phenylenediamine (5.2 mg, 0.05 mmol) in toluene (25 ml) was heated to reflux and kept at reflux for 24 h. The solvents were removed under reduced pressure and the residue was washed with water. The product was purified by column chromatography on silica gel with chloroform-methanol (1000:0.5, v/v) as eluent. The new main red fraction contained PO-PO. After recrystallization from chloroform and methanol, the product was collected as a red solid (31 mg, 30%). Mp. > 300 °C; ¹H NMR (300 MHz, CDCl₃, TMS): 8.24 (m, 8H), 7.37 (s, 4H), 7.22 (m, 16H), 6.83 (m, 16H), 4.11 (t, 4H),

1.67 (m, 4H), 1.42 (m, 4H), 1.28 (m, 72H), 0.93 (t, 6H). MS (MALDI-TOF): m/z , calculated for $C_{142}H_{134}N_4O_{16}$: 2152.6, found 2152.06 [M^+]. Elemental analysis (%) calculated for $C_{142}H_{134}N_4O_{16}$: C 79.23, H 6.27, N 2.60; found: C 78.28, H 6.28, N 2.59.

PO-PO-PO. The mixture of 1,6,7,12-tetra(4-*t*-butylphenoxy)perylene-3,4:9,10-tetracarboxylic acid anhydride (30 mg, 0.03 mmol) and excessive *N-n*-butyl-*N-p*-phenylenediamine-1,6,7,12-tetra(4-*t*-butylphenoxy)perylene-3,4:9,10-tetra carboxylic diimide **5** was heated to reflux and kept at reflux for 30 h. The solvents were removed under reduced pressure and the residue was washed with water. The product was purified by column chromatography on silica gel with chloroform-methanol (1000:0.5, v/v) as eluent. The new red fraction contained PO-PO-PO. After recrystallization from chloroform and methanol, the product was collected as a red solid (22 mg, 20%). Mp. > 300 °C; 1H NMR (300 MHz, $CDCl_3$, TMS): 8.24 (m, 12H), 7.37 (s, 8H), 7.22 (m, 24H), 6.83 (m, 24H), 4.11 (t, 4H), 1.67 (m, 4H), 1.41 (m, 4H), 1.28 (m, 108H), 0.93 (t, 6H). MS (MALDI-TOF): m/z , calculated for $C_{212}H_{194}N_6O_{24}$: 3209.83, found 3209.60 [M^+]. Elemental analysis (%) calculated for $C_{212}H_{194}N_6O_{24}$: C 79.33, H 6.09, N 2.62; found: C 79.01, H 6.05, N 2.56.

PO-PN. A mixture of *N-n*-butyl-*N-p*-phenylenediamine-1,6,7,12-tetra(4-*t*-butylphenoxy) perylene-3,4:9,10-tetracarboxylic diimide **5** (60 mg, 0.05 mmol), imidazole (600 mg), and *N-n*-butyl-1,7-di(pyrrolidinyl)perylene-3,4:9,10-tetracarboxylic-3,4-anhydride-9,10-imide **4** (29 mg, 0.05 mmol) in toluene (25 ml) was heated to reflux and kept at reflux for 24 h. The solvents were removed under reduced pressure and the residue was washed with water. The product was purified by column chromatography on silica gel with chloroform-methanol (1000:1.5, v/v) as eluent. The first purple fraction contained PO-PN. After recrystallization from chloroform and methanol, the product was collected as black solid (12 mg, 15%). Mp. > 300 °C; 1H NMR (300 MHz, $CDCl_3$, TMS): 8.47 (m, 4H), 8.24 (s + s, 4H), 7.75 (q, 2H), 7.46 (q, 4H), 7.25 (q, 8H), 6.84 (q, 8H), 4.24 (t, 2H), 4.12 (t, 2H), 3.77 (br, 4H), 2.86 (br, 4H), 2.00 (br, 8H), 1.75 (m, 2H), 1.67 (m, 2H), 1.48 (m, 2H), 1.44 (m, 2H), 1.28 (m, 36H), 0.99 (t, 3H), 0.94 (t, 3H); ^{13}C NMR (100 MHz, $CDCl_3$) δ 164.1, 164.0, 163.9, 163.4, 163.3, 156.1, 155.9, 152.9, 152.8, 147.3, 146.6, 146.4, 135.8, 135.0, 134.7, 134.2, 133.1, 133.0, 130.2, 130.1, 129.7, 129.5, 127.1, 126.6, 124.0, 123.7, 122.7, 122.6, 122.5, 122.1, 121.8, 121.1, 120.9, 120.7, 120.4, 119.8, 119.4, 119.3, 119.2, 119.1, 118.5, 117.9, 52.23, 40.4, 40.2, 34.4, 31.5, 30.3, 30.2, 29.7, 25.8, 20.4, 20.3, 13.9, 13.7. MS (MALDI-TOF): m/z , calculated for $C_{110}H_{100}N_6O_{12}$: 1698, found 1699.83 [M^+]. Elemental analysis (%) calculated for $C_{110}H_{100}N_6O_{12}$: C 77.81, H 5.94, N 4.95; found: C 78.01, H 5.87, N 4.65.

PO-PO-PN. A mixture of **6** (50 mg, 0.02 mmol), imidazole (600 mg), and *N-n*-butyl-*N-p*-phenylene diamine-1,7-di(pyrrolidinyl)perylene-3,4:9,10-tetracarboxylic diimide **9** (16 mg, 0.02 mmol) in toluene (25 ml) was heated to reflux and kept at reflux for 36 h. The solvents were removed under reduced pressure and the residue was washed with water. The product was purified by column chromatography on silica gel with chloroform-methanol (1000:2, v/v) as eluent. The third purple fraction contained PO-PO-PN. After recrystallization from chloroform and methanol, the product was collected as black solid (8 mg, 12%). Mp. > 300 °C; 1H NMR (300 MHz, $CDCl_3$, TMS): 8.49 (m, 4H), 8.26 (m, 8H), 7.74 (m, 2H),

7.47 (m, 4H), 7.38 (s, 4H), 7.23 (m, 16H), 6.84 (m, 16H), 4.23 (t, 2H), 4.09 (t, 2H), 3.78 (br, 4H), 2.85 (br, 4H), 1.73 (br, 8H), 1.67 (m, 2H), 1.64 (m, 2H), 1.46 (m, 2H), 1.41 (m, 2H), 1.28 (m, 72H), 0.99 (t, 3H), 0.95 (t, 3H). MS (MALDI-TOF): m/z , calculated for $C_{180}H_{160}N_8O_{20}$: 2755.24, found 2755.80 [M^+]. Elemental analysis (%) calculated for $C_{180}H_{160}N_8O_{20}$: C 78.47, H 5.85, N 4.07; found: C 78.51, H 5.95, N 4.01.

PO-PO-PO-PN. By employing the similar procedures of compound PO-PO-PN, using compound **8** (30 mg, 0.01 mmol) instead of **6** as starting material, compound PO-PO-PO-PN was prepared. The product was purified by column chromatography on silica gel with chloroform-methanol (1000:2, v/v) as eluent. The atropurpureus fraction contained PO-PO-PO-PN. After recrystallization from chloroform and methanol, the product was collected as a black solid (6 mg, 15%). Mp. > 300 °C; 1H NMR (300 MHz, $CDCl_3$, TMS): 8.47 (m, 4H), 8.25 (m, 12H), 7.77 (m, 2H), 7.46 (m, 4H), 7.39 (m, 8H), 7.23 (m, 24H), 6.84 (m, 24H), 4.24 (t, 2H), 4.11 (t, 2H), 3.78 (br, 4H), 2.88 (br, 4H), 2.03 (br, 8H), 1.75 (m, 4H), 1.39 (m, 4H), 1.28 (m, 108H), 0.99 (t, 3H), 0.95 (t, 3H). MS (MALDI-TOF): m/z , calculated for $C_{250}H_{220}N_{10}O_{28}$: 3812.47, found 3813.90 [M^+]. Elemental analysis (%) calculated for $C_{250}H_{220}N_{10}O_{28}$: C 78.76, H 5.82, N 3.67; found: C 78.40, H 5.89, N 3.63.

Results and discussion

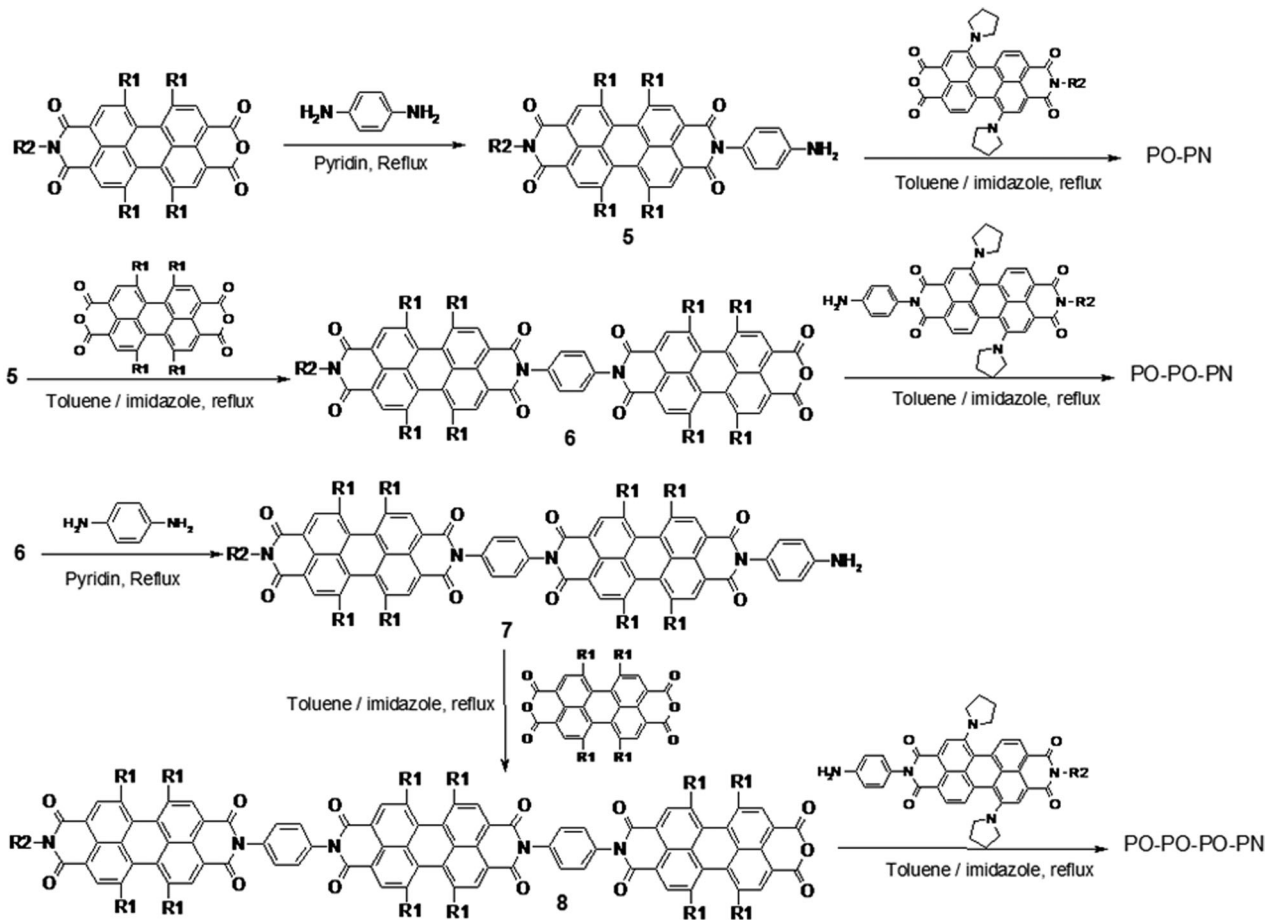
Molecular design and synthesis

Strong ground state interactions between different components in a molecular array always cause massive non-radiative decay for the excited states.⁵⁴⁻⁵⁶ These non-radiative decays compete with the energy transfer and fluorescence emission process in the molecular arrays, leading to low fluorescence quantum yields, and occasionally, short excitation hopping distance. To avoid this disadvantage, reducing the ground state interactions between the subunits in a molecular array will be a rational design. With this in mind, we designed these three compounds, PO-PN, PO-PO-PN, and PO-PO-PO-PN. We linked the PDI subunits with a phenyl group at the imide nitrogen positions. Because the frontier molecular orbital nodes of the PDI ring are on the imide nitrogen atoms, therefore, the interactions between the PDI subunits in these molecules should be small.⁶³ This weakly coupled molecular array also provides us with an opportunity to transfer excitation energy to a long distance with a small number of subunits.

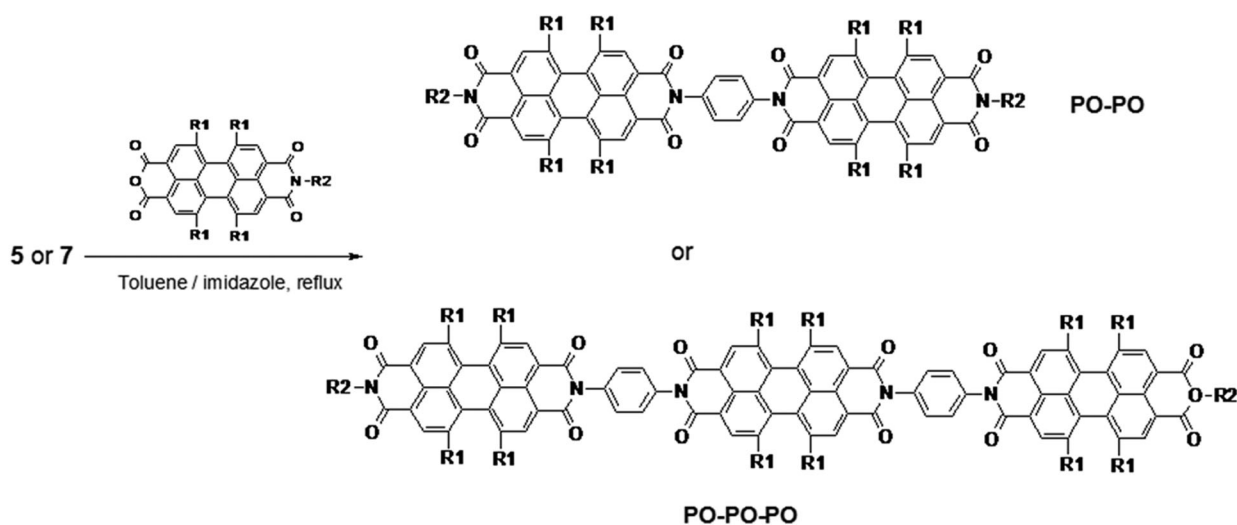
An overview of the synthetic procedures of the title compounds is shown in Scheme 2. The PDI molecules were connected to *p*-phenylenediamine *via* condensation of the corresponding amino compounds with the appropriate mono- or di-anhydride. All the new compounds were fully characterized with 1H NMR, MALDI-TOF mass spectra, as well as elemental analysis or ^{13}C NMR. For the purpose of comparison, two model compounds, namely, PO-PO and PO-PO-PO, were also prepared following similar procedures, Scheme 3.

Minimized molecular structure

The minimized structures of PO-PN, PO-PO-PN and PO-PO-PO-PN have been calculated on the level of B3LYP and 3-21G(d) basis set in the Gaussian 03 program package.⁶⁴ The energy



Scheme 2 Synthesis of PO-PN, PO-PO-PN, and PO-PO-PO-PN.



Scheme 3 Synthesis of model compounds PO-PO and PO-PO-PO.

minimized molecular structures of these linear molecules are given in Fig. 1. Due to steric repulsion between the phenoxy bay substituents, all the PDI subunits (both PO and PN) are no longer planar molecules but distort at a level of the central six

member ring.⁶⁵⁻⁶⁷ Fig. 1 also reveals that the PDI planes are almost perpendicular to the phenyl linkers due to the repulsion between the hydrogen atoms on the phenyl ring at *ortho* positions with the imide oxygen atoms of the PDI ring, and

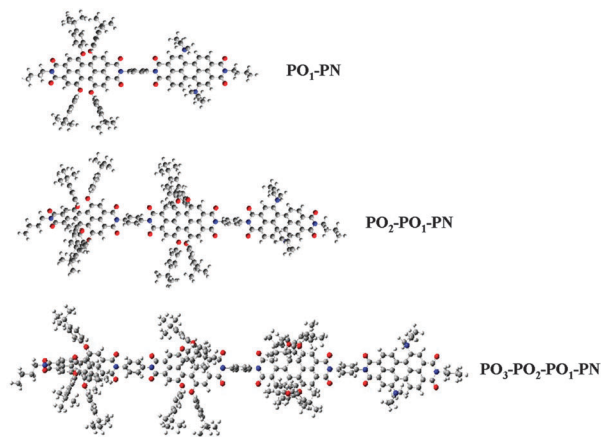


Fig. 1 Minimized molecular structure of the title compounds.

consequently, the different PDI subunits are roughly in the same plane and are almost parallel to each other. This co-planar conformation between the PDI subunits allows efficient energy transfer.

Absorption spectra

The electronic absorption spectra of PO–PN, PO–PO–PN and PO–PO–PO–PN together with that of their reference compounds (PO, PO–PO, PO–PO–PO) in CH_2Cl_2 are presented in Fig. 2.

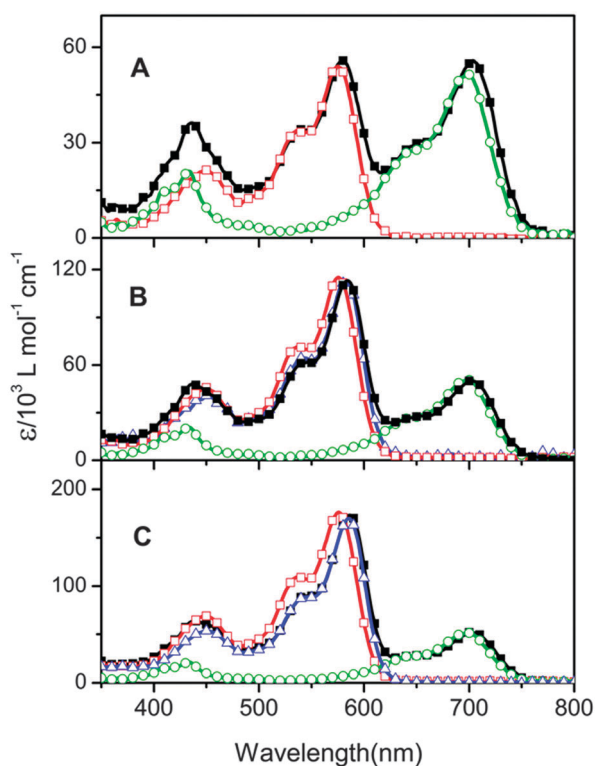


Fig. 2 UV-vis absorption spectra of compounds PO–PN (A, black line with solid square), PO–PO–PN (B, black line with solid square), PO–PO–PO–PN (C, black line with solid square) and the corresponding model compounds in CH_2Cl_2 . PO (red line with open square), PN (green line with open circle), PO–PO (B, blue line with open triangle), PO–PO–PO (C, blue line with open triangle).

Fig. 2A compares the absorption spectra of PO–PN with that of monomer PO and PN. The spectrum of PO–PN is almost identical to that of the 1 : 1 mixture of PO and PN. This result indicates that no strong ground state interactions exist between PO and PN units in this molecule. A very small shift of the absorption maxima of the PO (1 nm) and PN (2 nm) units of PO–PN in comparison with that of monomeric PO and PN can be identified. This might be attributed to a weak ground state interaction between the PO and PN units. The absorption spectra of PO–PO–PN, Fig. 2B, presents the maximal absorption band at 585 nm, which can be attributed to the absorption of PO subunits. Compared with that of monomeric PO, the peak position red-shifted for about 5 nm, which is obviously larger than that observed for the PO subunit in PO–PN. The spectra of PO–PO–PN at this part are also identical to that of model PO–PO. This result suggests that there are weak “head to tail” interactions between the PO subunits in PO–PO–PN and PO–PO at ground states.³⁹ Similar results can also be deduced from the absorption spectra of PO–PO–PO–PN and PO–PO–PO. Moreover, the absorbance of these three compounds at 572 nm increases linearly along with the increase on the number of PO subunits, which suggests further that the ground state interactions between the PO subunits within these three compounds are weak.

Table 1 summarizes the UV/vis absorption properties of these compounds in CH_2Cl_2 and toluene. The absorption spectra of these compounds in toluene and in CH_2Cl_2 are almost identical except a slight bathochromic shift of a few nanometres when going from toluene to CH_2Cl_2 . This can be attributed to the stabilizing effect of the larger polarity of CH_2Cl_2 to the excited states.

Fluorescence spectra

Fig. 3A shows the fluorescence spectra of PO–PN in CH_2Cl_2 with excitation at 510 nm. The absorbance of PO is seven times larger than that of PN at this wavelength, therefore, the excitation at 510 nm is roughly considered to be a selective excitation to the PO subunits.

As expected, the fluorescence of the PO unit in PO–PN appears around 610 nm, which is extremely small. This indicates that the fluorescence of PO in PO–PN is quenched significantly. The strong emission band centred at about 743 nm can be attributed to the fluorescence of the PN unit, which suggests the presence of photoinduced energy transfer from PO to PN within PO–PN. The excitation spectrum of PO–PN, Fig. 4, shows a pronounced PO absorption feature in the region of 500–625 nm. This observation suggests that the absorption of PO contributes to the fluorescence of PN to a remarkable extent and indicates the presence of singlet–singlet energy transfer from PO to PN within PO–PN. Similar results can be deduced from the fluorescence spectra (Fig. S1 and S2 in ESI†) and excitation spectra (Fig. 4) of PO–PO–PN and PO–PO–PO–PN. After normalization at 710 nm, the excitation spectra of PO–PN, PO–PO–PN, and PO–PO–PO–PN revealed that the peak intensity at about 580 nm increases linearly along with the increase on the number of PO subunits within one molecule

Table 1 The UV-vis absorption properties of the compounds

Compound	λ [nm] ($\epsilon/10^4$ L mol ⁻¹ cm ⁻¹)	
	Toluene	CH ₂ Cl ₂
PO	447(2.00), 530(3.60), 571(6.00)	447(2.00), 535(3.20), 574(5.20)
PN	428(1.60), 683(4.40)	432(1.80), 698(4.80)
PO-PN	430(3.20), 532(3.00), 572(5.20), 685(4.80)	434(3.40), 535(3.20), 578(5.40), 703(5.40)
PO-PO-PN	431(4.48), 534(5.70), 576(10.7), 687(4.82)	436(4.77), 542(6.13), 582(11.2), 702(4.96)
PO-PO-PO-PN	432(6.00), 539(8.31), 579(16.4), 688(4.98)	436(6.39), 543(8.94), 583(17.2), 703(5.13)

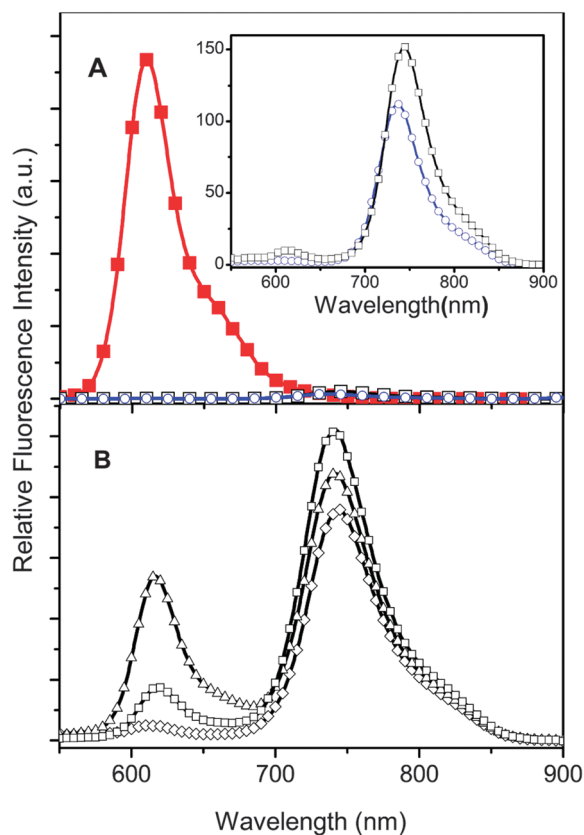


Fig. 3 (A) Fluorescence spectra of PO-PN (black line with open squares), PO (red line with closed squares), PN (blue line with open circles) in CH₂Cl₂, $\lambda_{\text{ex}} = 510$ nm for PO and PO-PN, $\lambda_{\text{ex}} = 650$ nm for PN, [PO-PN] = [PO] = [PN] = 5×10^{-6} mol L⁻¹. The inset shows the expanded spectra for PN and PO-PN. (B) Fluorescence spectra of PO-PN (open squares), PO-PO-PN (open diamonds), PO-PO-PO-PN (open triangles) in CH₂Cl₂, $\lambda_{\text{ex}} = 510$ nm.

(inset of Fig. 4), this suggests that all the PO subunits in these compounds contribute equally to the energy transfer to PN.

Fig. 3B compares the fluorescence spectra of PO-PN with that of PO-PO-PN and PO-PO-PO-PN when they were excited at 510 nm. The fluorescence of PO at about 611 nm can be found in all these fluorescence spectra, which suggests that the singlet-singlet energy transfer from PO to PN in these three compounds is not 100%. For the purpose of estimating the energy transfer efficiencies quantitatively, the fluorescence quantum yields of these three compounds together with the model compounds are measured. The results are summarized in Table 2.

The fluorescence quantum yield has a value of about 0.8 for PO in toluene, whereas for PO-PO and PO-PO-PO the

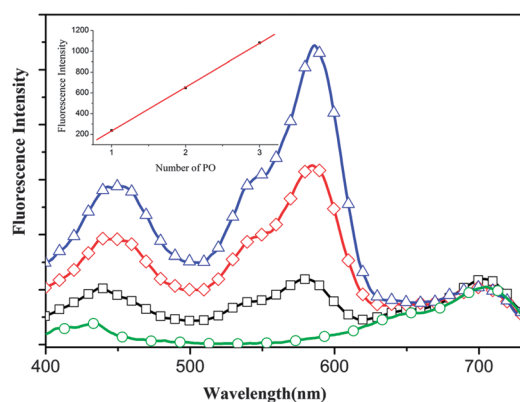


Fig. 4 The normalized excitation spectra of PO-PN (black line with open squares), PO-PO-PN (red line with open diamonds), PO-PO-PO-PN (blue line with open triangles) monitoring at 750 nm compared with the absorption spectra of PN (green line with open circles) in CH₂Cl₂. The inset shows the plot of fluorescence intensity at 580 nm against the number of PO subunits in a molecule.

Table 2 Fluorescence properties of the compounds (excited at 510 nm)

Compound	Φ_f (%)		Φ_q (%)		τ_f (ns) Toluene
	Toluene	CH ₂ Cl ₂	Toluene	CH ₂ Cl ₂	
PO	81.1	80.2	—	—	6.59
PO-PO	60.6	62.5	—	—	5.65
PO-PO-PO	50.8	46.2	—	—	5.46
PO-PN	0.28 ^a	0.15 ^a	99.7	99.8	—
PO-PO-PN	0.58 ^a	0.61 ^a	99.1	99.1	—
PO-PO-PO-PN	0.15 ^a	0.15 ^a	99.7	99.7	—

^a Fluorescence quantum yields of PO components.

fluorescence quantum yields drop to a value of about 0.6 and 0.5, respectively. As indicated before, the presence of the phenyl bridges introduces some flexibility in the structure and opens up new radiationless deactivation channels for the excited states.⁶⁸

The efficiencies of the fluorescence quenching (Φ_q) of PO by PN within PO-PN, PO-PO-PN, PO-PO-PO-PN are calculated based on the fluorescence quantum yields of PO within these compounds following eqn (1):⁶⁹

$$\Phi_q = 1 - \Phi_f/\Phi_0 \quad (1)$$

where Φ_f is the fluorescence quantum yield of PO within PO-PN, PO-PO-PN, PO-PO-PO-PN and Φ_0 represents the fluorescence quantum yields of the model compounds PO, PO-PO and

PO-PO-PO. The calculated results (Table 2) indicate that fluorescence quenching efficiency in all these three compounds is larger than 99% and close to quantitative. This also suggests that the energy transfer from PO to PN in these three compounds is extremely efficient.

Fluorescence lifetime

The fluorescence lifetimes at 611 nm of these three compounds are measured with time related single-photon counting methods (TSPC). The results are summarized in Table 2. The fluorescence lifetime measured for the model compound PO in toluene is 6.59 ns, which is similar to those in the literature.⁶⁷ For model compounds PO-PO and PO-PO-PO in toluene, the dominating component in the fluorescence decay is 5.65 and 5.46 ns, respectively. The remaining small fraction (with an amplitude less than 5%) is attributed to a conformational relaxation of the bay substituents.⁶⁷ It is interesting that the fluorescence lifetimes of PO-PO and PO-PO-PO are generally shorter than that of model compound PO. This is probably due to the opening up of additional radiationless decay pathways in these two compounds and is in agreement with the drop in fluorescence quantum yields. This result is similar with that observed for a diphenylacetylene linked PDI trimer.⁵³ The fluorescence lifetimes of PO subunits at 611 nm in PO-PN, PO-PO-PN, and PO-PO-PO-PN can not be measured accurately by TSPC method due to the very weak emission intensities.

Förster type energy transfer processes

The spectral overlap between the emission spectrum and ground-state absorption spectrum (Fig. 5) indicates that two kinds of energy transfer processes are theoretically possible within these three compounds: (i) an energy hopping between PO subunits, which is energy transfer from the S_1 state toward the ground-state of a neighbour PO, and (ii) the energy transfer from PO to PN. Moreover, the spectral overlap between the emission of PO and the absorption of PO as shown in Fig. 5A is smaller than that between the emission of PO and the absorption of PN as shown in Fig. 5B. Both processes can be evaluated within the framework of Förster theory. The critical distance R_0 can be calculated from a few parameters obtained experimentally, namely the spectral overlap integral J between the donor emission (corresponding to the PO S_1 - S_0 transition) and acceptor absorption spectrum, and the relative orientation of the two dipoles expressed by the orientation factor κ^2 . The detailed calculation procedures are shown in the ESI† and the results are displayed in Table 3. Here, the orientation factor is assumed to have the maximum value $\kappa^2 = 4$ as the transition dipoles are quasi collinearly oriented and the S_0 - S_1 transition is oriented along the long molecular axis.⁷⁰

The Förster type energy transfer efficiencies (Φ_{EnT}) from PO to PN as well as that between the neighbour PO subunits within these three compounds are estimated (eqn (S2) and (S3) in ESI†).⁵³ The results are summarized in Table 3. Obviously, the energy transfer between neighbour POs as well as between directly connected PO and PN is very efficient. This corresponds well with the experimentally measured high fluorescence

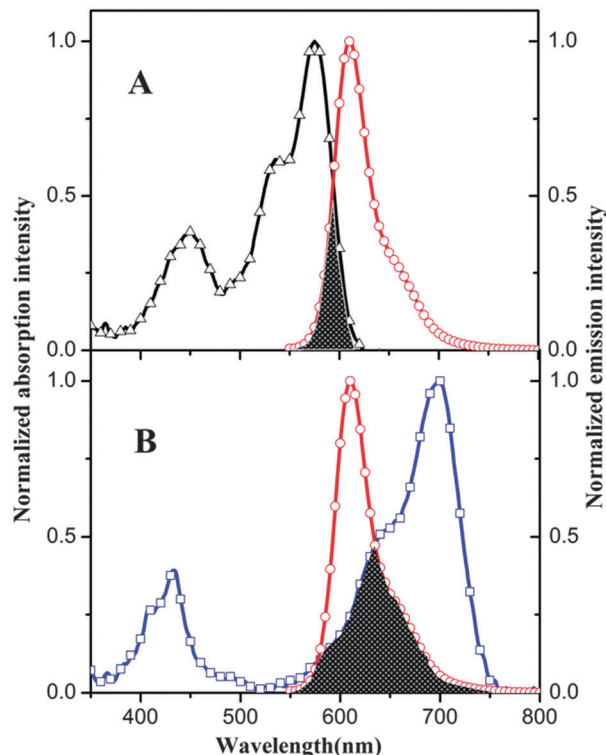


Fig. 5 (A) Spectral overlap (gray shadow in the spectra) of the fluorescence (red line with open circles) and ground-state absorption (black line with open triangles) relevant for the energy hopping process between PO and PO in CH_2Cl_2 . (B) Spectral overlap (gray shadow in the spectra) of the fluorescence (red line with open circles) of PO and ground-state absorption (blue line with open square) band of PN relevant for the energy transfer process from PO to PN in CH_2Cl_2 .

Table 3 Estimated Förster type energy transfer parameters within these compounds in toluene^a

Donor-acceptor pair	R_0 (Å)	J ($\text{mol}^{-1} \text{dm}^3 \text{cm}^{-1} \text{nm}^4$)	R^e (Å)	Φ_{EnT} (%)
PO-PO	34.5	7.8×10^{13}	16.93	98.6
PO ₁ -PN ^b	40.7	2.1×10^{14}	16.93	99.5
PO ₂ -PO-PN ^c	40.7	2.1×10^{14}	33.86	75.1
PO ₃ -PO-PO-PN ^d	40.7	2.1×10^{14}	50.79	21.0

^a The calculation methods as well as the formulas are shown in the ESI. ^b The energy transfer from the directly connected PO to PN. ^c The energy transfer from the second PO subunit to PN. ^d The energy transfer from the third PO subunit to PN. ^e The centre to centre distance between donor and acceptor read from the minimized structure.

quenching efficiency in PO-PN as shown in Table 2. However, the calculated Φ_{EnT} for the energy transfer from PO to PN which are not connected directly are significantly smaller than that in PO-PN. This means the direct energy transfer from the second and the third PO subunits within PO-PO-PN and PO-PO-PO-PN to PN unit should be less efficient. If there was no energy hopping between the PO subunits within PO-PO-PN and PO-PO-PO-PN, the total energy transfer efficiency in these two compounds should be small. This is obviously controversial to the measured high fluorescence quenching efficiencies for these two compounds as shown in Table 2. This result

suggests that efficient energy hopping between neighbour PO subunits within PO-PO-PN and PO-PO-PO-PN is involved in the energy transfer process in these two compounds. Because the energy hopping efficiency between PO subunits is also efficient and quick, therefore, the total energy transfer efficiency from PO to PN within PO-PO-PN and PO-PO-PO-PN is also efficient.

Transient absorption spectra

To determine the rate constants for the energy transfer from PO to PN within PO-PN, PO-PO-PN and PO-PO-PO-PN, femtosecond absorption spectra of these compounds in toluene were recorded (ESI†). The transient absorption spectra of all these three compounds are featured similarly with two ground state bleaching bands at 588 nm and 710 nm, corresponding to the ground state absorption of PO and PN subunits, respectively.

The decay traces of the ground states bleaching of PO-PN along with time delay are shown in Fig. 6. Fitting the decay traces of the ground state bleaching at 588 nm, which corresponds to the absorption of PO, gives three time constants, 252 fs, 1.59 ps, and 344.5 ps, with the shortest component (80% in amplitude) dominating the decay of the excited states of PO within PO-PN. The fitting on the decay of the ground state bleaching of PN at 710 nm gives two components, a rising component with a time constant of 236 fs and a decay component with a time constant of 368.7 ps. The rising component of

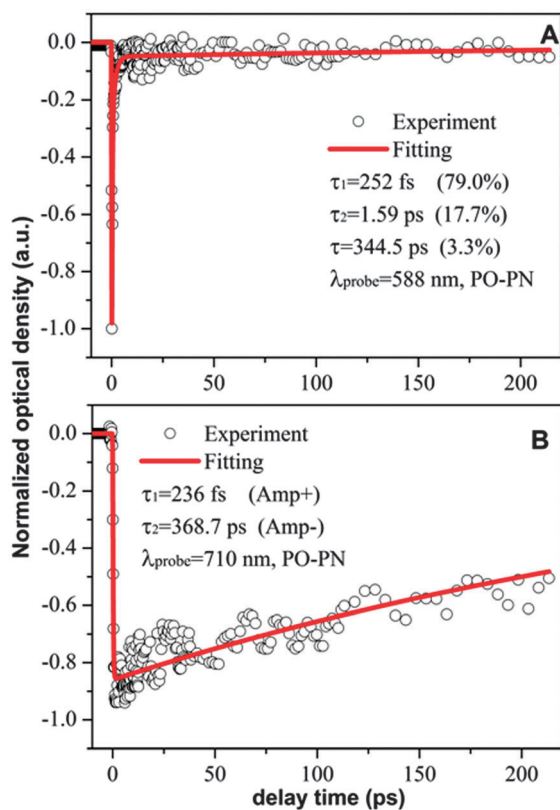


Fig. 6 The decay traces of the ground state bleaching of PO-PN at 588 nm (A) and 710 nm (B) and the fitting results (excited at 530 nm with a 120 fs pulse of light).

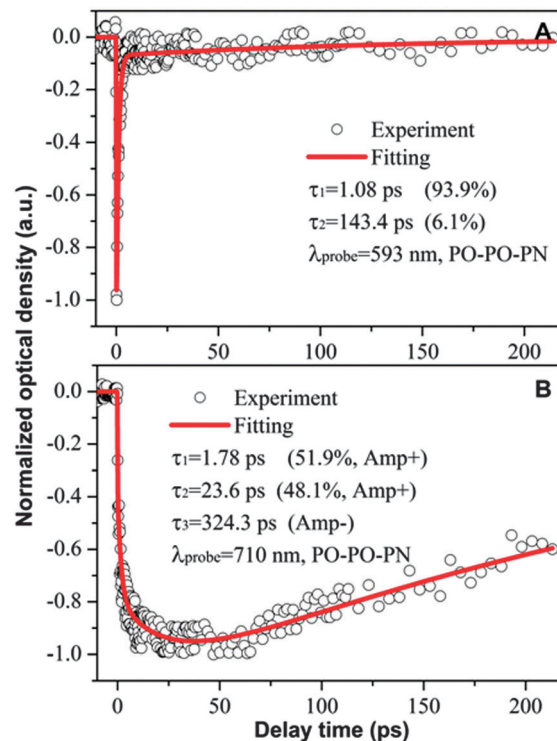


Fig. 7 The decay traces of the ground state bleaching of PO-PO-PN at 593 nm (A) and 710 nm (B) and the fitting results (excited at 530 nm with a 120 fs pulse of light).

PN corresponds very well with the shortest decay component of PO, which can be attributed to the energy transfer from PO to PN in PO-PN. The other two minor decay components of PO can be attributed to an intramolecular vibrational redistribution (IVR), which were previously found for other PDI derivatives.⁶⁷ Similar fitting on the decay traces of the ground state bleaching of PO-PO-PN at 588 nm retrieved two components, a fast component of 1.08 ps (94%) and a slow component of 143.4 ps (6%), Fig. 7. The decay traces at 710 nm, corresponding to the ground state bleaching of the PN unit within PO-PO-PN, revealed three components with two rising components and one decaying component. The two rising components have lifetimes of 1.78 ps (52%) and 23.6 ps (48%), respectively. Obviously, these two rising components can be attributed to two different energy transfer processes from PO to PN within PO-PO-PN. The decay components of PO at 588 nm do not correspond well with the rising of PN at 710 nm, which suggests a more complicated energy transfer mechanism in this compound. The fitting results also suggest that the energy transfer from PO to PN within PO-PO-PN (1.78 ps and 23.6 ps) is slower than that in PO-PN (236 fs).

The transient absorption experiments on PO-PO-PO-PN give similar results as that of PO-PO-PN (ESI†). Two decay components with lifetimes of 777 fs and 6.39 ps, respectively, were found for the ground state bleaching of PO at 580 nm. The decay of PN at 710 nm gives two rising components with lifetimes of 1.39 and 9.67 ps, respectively, and a decay lifetime of 680.1 ps. The two rising lifetimes can be attributed to the

energy transfer from PO to PN. Again, the uncoordinated decay of the ground state bleaching of PO and PN within PO–PO–PO–PN suggests a more complicated energy transfer mechanism as mentioned above and the energy transfer from PO to PN within PO–PO–PO–PN is slower than that in PO–PN. More importantly, even though the long distance between PO and PN in PO–PO–PO–PN, the rate constants for the energy transfer from PO to PN is very fast and close to that of the energy transfer from B800 to B850 in the light harvesting system (LH II) of photosynthesis.⁷¹

Conclusions

We have successfully synthesized a series of rigid and linear PDI based donor–acceptor oligomers linked by phenyl bridges. In these compounds, the PO subunits interacted with each other weakly as revealed by the UV-vis absorption spectra. But when the PO subunits are selectively excited, intramolecular energy transfer proceeds efficiently from the excited PO subunits to the PN unit with efficiency higher than 99%. Both the theoretical predication and transient absorption studies suggest that the energy hopping among the PO subunits has involved in the energy transfer from PO to PN. This research suggests that the weakly interacted organic dye molecules can serve as photon carriers, which can transfer the excitation energy to a large distance without a significant decrease in efficiency. These molecules also partially mimicked the energy transfer within LH I and LH II. This result is also meaningful for the design of new fluorescence sensors with high sensitivity because the excitation energy transfer in the PO oligomer might be employed to amplify the fluorescence quenching efficiency and thus increase the sensitivity.

Acknowledgements

We thank the Natural Science Foundation of China (grand no. 21073112, 21173136, 91233108 and 21173063), the National Basic Research Program of China (973 Program: 2012CB93280) and the Natural Science foundation of Shandong Province (ZR2010EZ007) for financial support.

References

- R. E. Blankenship, *Molecular Mechanisms of Photosynthesis*, Blackwell Science, Oxford, 2002.
- K. N. Ferreira, T. M. Iverson, K. Maghlaoui, J. Barber and S. Iwata, *Science*, 2004, **303**, 1831–1838.
- J. Deisenhofer, O. Epp, K. Miki, R. Huber and H. Michel, *J. Mol. Biol.*, 1984, **180**, 385–398.
- J. P. Allen, G. Feher, T. O. Yeates, H. Komiya and D. C. Rees, *Proc. Natl. Acad. Sci. U. S. A.*, 1987, **84**, 5730–5743.
- C. H. Chang, O. El-Kabban, D. Tiede, J. Norris and M. Schiffer, *Biochemistry*, 1991, **30**, 5352–5360.
- M. R. Wasielewski, *J. Org. Chem.*, 2006, **71**, 5051–5066.
- V. Balzani and F. Scandola, *Supramolecular Photochemistry*, Ellis Horwood, Chichester, 1991.
- J. L. Sessler, B. Wang, S. L. Springs and C. T. Brown, *Comprehensive Supramolecular Chemistry*, ed. J. L. Atwood, J. E. D. Davies, D. D. MacNicol, F. Vogtle and Y. Murakami, Pergamon, Oxford, 1996, vol. 4, pp. 311–336.
- C. J. Chang, J. D. Brown, M. C. Y. Chang, E. A. Baker and D. G. Nocera, *Electron Transfer in Chemistry*, ed. V. Balzani, Wiley-VCH, Weinheim, 2001, vol. 3, pp. 409–461.
- F. J. M. Hoeben, P. Jonkheijm, E. W. Meijer and A. P. H. J. Schenning, *Chem. Rev.*, 2005, **105**, 1491–1546.
- H.-J. Son, S. Jin, S. Patwardhan, S. J. Wezenberg, N. C. Jeong, M. So, C. E. Wilmer, A. A. Sarjeant, G. C. Schatz, R. Q. Snurr, O. K. Farha, G. P. Wiederrecht and J. T. Hupp, *J. Am. Chem. Soc.*, 2013, **135**, 862–869.
- Y. Nakamura, N. Aratani and A. Osuka, *Chem. Soc. Rev.*, 2007, **36**, 831–845.
- R. F. Kelly, R. H. Goldsmith and M. R. Wasielewski, *J. Am. Chem. Soc.*, 2007, **129**, 6384–6385.
- Y. Kubo, Y. Kitada, R. Wakabayashi, T. Kishida, M. Ayabe, K. Kaneko, M. Takeuchi and S. Shinkai, *Angew. Chem., Int. Ed.*, 2006, **45**, 1–7.
- I. W. Hwang, M. Park, T. K. Ahn, Z. S. Yoon, D. M. Ko, D. Kim, F. Ito, Y. Ishibashi, S. R. Khan, Y. Nagasawa, H. Miyasaka, C. Ikeda, R. Takahashi, K. Ogawa, A. Satake and Y. Kobuke, *Chem.–Eur. J.*, 2005, **11**, 3753–3761.
- Y. Nakamura, I. W. Hwang, N. Aratani, T. K. Ahn, D. M. Ko, A. Takagi, T. Kawai, T. Matsumoto, D. Kim and A. Osuka, *J. Am. Chem. Soc.*, 2005, **127**, 236–246.
- M. Hoffmann, J. Karnbratt, M. H. Chang, L. M. Herz, B. Albinsson and H. L. Anderson, *Angew. Chem., Int. Ed.*, 2008, **47**, 4993–4996.
- M. Hoffmann, C. J. Wilson, B. Odell and H. L. Anderson, *Angew. Chem., Int. Ed.*, 2007, **46**, 3122–3125.
- O. Mongin, A. Schuwey, M. A. Vallot and A. Gossauer, *Tetrahedron Lett.*, 1999, **40**, 8347–8350.
- J. Z. Li, A. Ambroise, S. I. Yang, J. R. Diers, J. Seth, C. R. Wack, D. F. Bocian, D. Holten and J. S. Lindsey, *J. Am. Chem. Soc.*, 1999, **121**, 8927–8940.
- R. W. Wagner, J. Seth, S. I. Yang, D. Kim, D. F. Bocian, D. Holten and J. S. Lindsey, *J. Org. Chem.*, 1998, **63**, 5042–5049.
- N. Aratani and A. Osuka, *Chem. Commun.*, 2008, 4067–4069.
- A. Vidal-Ferran, Z. Clyde-Watson, N. Bampos and J. K. M. Sanders, *J. Org. Chem.*, 1997, **62**, 240–241.
- S. Rucareanu, O. Mongin, A. Schuwey, N. Hoyler, A. Gossauer, W. Amrein and H.-U. Hediger, *J. Org. Chem.*, 2001, **66**, 4973–4988.
- R. W. Wagner, J. S. Lindsey, J. Seth, V. Palaniappan and D. F. Bocian, *J. Am. Chem. Soc.*, 1996, **118**, 3996–3997.
- N. Nagata, Y. Kuramochi and Y. Kobuke, *J. Am. Chem. Soc.*, 2009, **131**, 10–11.
- C. Jung, B. K. Müller, D. C. Lamb, F. Nolde, K. Müllen and C. Bräuchle, *J. Am. Chem. Soc.*, 2006, **128**, 5283–5291.
- R. Metivier, F. Nolde, K. Müllen and T. Basche, *Phys. Rev. Lett.*, 2007, **98**, 047802.
- J. Kirstein, B. Platschek, C. Jung, R. Brown, T. Bein and C. Bräuchle, *Nat. Mater.*, 2007, **6**, 303–310.

- 30 M. R. Wasielewski, *Acc. Chem. Res.*, 2009, **42**, 1910–1921.
- 31 C. Hippus, I. H. M. van Stokkum, M. Gsanger, M. M. Groeneveld, R. M. Williams and F. Würthner, *J. Phys. Chem. C*, 2008, **112**, 2476–2486.
- 32 M. J. Ahrens, L. E. Sinks, B. Rybtchinski, W. H. Liu, B. A. Jones, J. M. Giaimo, A. V. Gusev, A. J. Goshe, D. M. Tiede and M. R. Wasielewski, *J. Am. Chem. Soc.*, 2004, **126**, 8284–8294.
- 33 M. W. Holman, R. C. Liu and D. M. Adams, *J. Am. Chem. Soc.*, 2003, **125**, 12649–12654.
- 34 R. Yasukuni, T. Asahi, T. Sugiyama, H. Masuhara, M. Sliwa, J. Hofkens, F. C. De Schryver, M. Van der Auweraer, A. Herrmann and K. Muller, *Appl. Phys. A: Mater. Sci. Process.*, 2008, **93**, 5–9.
- 35 T. van der Boom, R. T. Hayes, Y. Y. Zhao, P. J. Bushard, E. A. Weiss and M. R. Wasielewski, *J. Am. Chem. Soc.*, 2002, **124**, 9582–9590.
- 36 J. Q. Feng, Y. X. Zhang, C. T. Zhao, R. J. Li, W. Xu, X. Y. Li and J. Z. Jiang, *Chem.–Eur. J.*, 2008, **14**, 7000–7010.
- 37 J. M. Giaimo, J. V. Lockard, L. E. Sinks, A. M. Scott, T. M. Wilson and M. R. Wasielewski, *J. Phys. Chem. A*, 2008, **112**, 2322–2330.
- 38 H. Yoo, J. Yang, A. Yousef, M. R. Wasielewski and D. Kim, *J. Am. Chem. Soc.*, 2010, **132**, 3939–3944.
- 39 T. Ishi-i, K. Murakami, Y. Imai and S. Mataka, *J. Org. Chem.*, 2006, **71**, 5752–5760.
- 40 H. Langhals and J. Gold, *J. Prakt. Chem.*, 1996, **338**, 654–659.
- 41 P. Tinnefeld, K. D. Weston, T. Vosch, M. Cotlet, T. Weil, J. Hofkens, K. Müllen, F. C. De Schryver and M. Sauer, *J. Am. Chem. Soc.*, 2002, **124**, 14310–14311.
- 42 T. Gensch, J. Hofkens, A. Heirmann, K. Tsuda, W. Verheijen, T. Vosch, T. Christ, T. Basche, K. Müllen and F. C. De Schryver, *Angew. Chem., Int. Ed.*, 1999, **38**, 3752–3756.
- 43 J. Hofkens, M. Maus, T. Gensch, T. Vosch, M. Cotlet, F. Kohn, A. Herrmann, K. Müllen and F. C. De Schryver, *J. Am. Chem. Soc.*, 2000, **122**, 9278–9288.
- 44 M. Maus, R. De, M. Lor, T. Weil, S. Mitra, U. M. Wiesler, A. Herrmann, J. Hofkens, T. Vosch, K. Müllen and F. C. De Schryver, *J. Am. Chem. Soc.*, 2001, **123**, 7668–7676.
- 45 T. Vosch, J. Hofkens, M. Cotlet, F. Kohn, H. Fujiwara, R. Gronheid, K. Van Der Biest, T. Weil, A. Herrmann, K. Müllen, S. Mukamel, M. Van der Auweraer and F. C. De Schryver, *Angew. Chem., Int. Ed.*, 2001, **40**, 4643–4648.
- 46 T. Vosch, M. Cotlet, J. Hofkens, K. Van der Biest, M. Lor, K. Weston, P. Tinnefeld, M. Sauer, L. Latterini, K. Müllen and F. C. De Schryver, *J. Phys. Chem. A*, 2003, **107**, 6920–6931.
- 47 S. Masuo, T. Vosch, M. Cotlet, P. Tinnefeld, S. Habuchi, T. D. M. Bell, I. Oesterling, D. Beljonne, B. Champagne, K. Müllen, M. Sauer, J. Hofkens and F. C. De Schryver, *J. Phys. Chem. B*, 2004, **108**, 16686–16696.
- 48 W. Schroyers, R. Vallee, D. Patra, J. Hofkens, S. Habuchi, T. Vosch, M. Cotlet, K. Müllen, J. Enderlein and F. C. De Schryver, *J. Am. Chem. Soc.*, 2004, **126**, 14310–14311.
- 49 J. P. Hoogenboom, E. M. H. P. van Dijk, J. Hernando, N. F. van Hulst and M. F. Garcia-Parajo, *Phys. Rev. Lett.*, 2005, **95**, 097401.
- 50 J. P. Hoogenboom, J. Hernando, E. van Dijk, N. F. van Hulst and M. F. Garcia-Parajo, *ChemPhysChem*, 2007, **8**, 823–833.
- 51 J. Hernando, J. P. Hoogenboom, E. M. H. P. van Dijk, J. J. Garcia-Lopez, M. Crego-Calama, D. N. Reinhoudt, N. F. van Hulst and M. F. Garcia-Parajo, *Phys. Rev. Lett.*, 2004, **93**, 236404.
- 52 J. Hernando, E. M. H. P. van Dijk, J. P. Hoogenboom, J.-J. Garcia-Lopez, D. N. Reinhoudt, M. Crego-Calama, M. F. Garcia-Parajo and N. F. van Hulst, *Phys. Rev. Lett.*, 2006, **97**, 216403.
- 53 T. Vosch, E. Fron, J.-i. Hotta, A. Deres, H. Uji-i, A. Idrissi, J. Yang, D. Kim, L. Puhl, A. Haeuseler, K. Müllen, F. C. De Schryver, M. Sliwa and J. Hofkens, *J. Phys. Chem. C*, 2009, **113**, 11773–11782.
- 54 K. Sugiyasu, N. Fujita and S. Shinkai, *Angew. Chem., Int. Ed.*, 2004, **43**, 1229.
- 55 C. Hippus, F. Schlosser, M. O. Vysotsky, V. Böhmer and F. Würthner, *J. Am. Chem. Soc.*, 2006, **128**, 3870–3871.
- 56 X. Li, L. E. Sinks, B. Rybtchinski and M. R. Wasielewski, *J. Am. Chem. Soc.*, 2004, **126**, 10810–10811.
- 57 B. Rybtchinski, L. E. Sinks and M. R. Wasielewski, *J. Am. Chem. Soc.*, 2004, **126**, 12268–12269.
- 58 A. S. Lukas, Y. Zhao, S. E. Miller and M. R. Wasielewski, *J. Phys. Chem. B*, 2002, **106**, 1299–1306.
- 59 L. E. Sinks, B. Rybtchinski, M. Iimura, B. A. Jones, A. J. Goshe, X. Zuo, D. M. Tiede, X. Li and M. R. Wasielewski, *Chem. Mater.*, 2005, **17**, 6295–6303.
- 60 J. M. Giaimo, A. V. Gusev and M. R. Wasielewski, *J. Am. Chem. Soc.*, 2002, **124**, 8530–8531.
- 61 F. Würthner, C. Thalacker, A. Sautter, W. Schrtl, W. Ibach and O. Hollricher, *Chem.–Eur. J.*, 2000, **6**, 3871–3886.
- 62 Y. Du, L. Jiang, J. Zhou, G. Qi and X. Li, *Org. Lett.*, 2012, **14**, 3052–3055.
- 63 B. Liang, Y. Zhang, Y. Wang, W. Xu and X. Li, *J. Mol. Struct.*, 2009, **917**, 133–141.
- 64 M. J. Frisch, G. W. Trucks, H. B. Schlegel, G. E. Scuseria, M. A. Robb, J. R. Cheeseman, J. A. Montgomery, Jr., T. Vreven, K. N. Kudin, J. C. Burant, J. M. Millam, S. S. Iyengar, J. Tomasi, V. Barone, B. Mennucci, M. Cossi, G. Scalmani, N. Rega, G. A. Petersson, H. Nakatsuji, M. Hada, M. Ehara, K. Toyota, R. Fukuda, J. Hasegawa, M. Ishida, T. Nakajima, Y. Honda, O. Kitao, H. Nakai, M. Klene, X. Li, J. E. Knox, H. P. Hratchian, J. B. Cross, C. Adamo, J. Jaramillo, R. Gomperts, R. E. Stratmann, O. Yazyev, A. J. Austin, R. Cammi, C. Pomelli, J. W. Ochterski, P. Y. Ayala, K. Morokuma, G. A. Voth, P. Salvador, J. J. Dannenberg, V. G. Zakrzewski, S. Dapprich, A. D. Daniels, M. C. Strain, O. Farkas, D. K. Malick, A. D. Rabuck, K. Raghavachari, J. B. Foresman, J. V. Ortiz, Q. Cui, A. G. Baboul, S. Clifford, J. Cioslowski, B. B. Stefanov, G. Liu, A. Liashenko, P. Piskorz, I. Komaromi, R. L. Martin, D. J. Fox, T. Keith, M. A. Al-Laham, C. Y. Peng, A. Nanayakkara, M. Challacombe, P. M. W. Gill, B. Johnson, W. Chen, M. W. Wong, C. Gonzalez and J. A. Pople, *Gaussian 03, Revision B.05*, Gaussian, Inc., Pittsburgh, PA, 2003.
- 65 J. Hofkens, T. Vosch, M. Maus, F. Kohn, M. Cotlet, T. Weil, A. Herrmann, K. Müllen and F. C. De Schryver, *Chem. Phys. Lett.*, 2001, **333**, 255–263.

- 66 P. Osswald and F. Würthner, *J. Am. Chem. Soc.*, 2007, **129**, 14319–14326.
- 67 E. Fron, G. Schweitzer, P. Osswald, F. Würthner, P. Marsal, D. Beljonne, K. Mullen, F. C. De Schryver and M. Van der Auweraer, *Photochem. Photobiol. Sci.*, 2008, **7**, 1509–1521.
- 68 M. W. Holman, R. Liu, L. Zang, P. Yan, S. A. DiBenedetto, R. D. Bowers and D. M. Adams, *J. Am. Chem. Soc.*, 2004, **126**, 16126–16133.
- 69 N. J. Turro, *Modern Molecular Photochemistry*, Benjamin/Cummings, Menlo Park, 1978.
- 70 H. Langhals, A. J. Esterbauer, A. Walter, E. Riedle and I. Pugliesi, *J. Am. Chem. Soc.*, 2010, **132**, 16777–16782.
- 71 X. Chen, L. Zhang, Y. Weng, L. Du, M. Ye, G. Yang, R. Fujii, F. S. Rondonuwu, Y. Koyama, S. Wu and J. Zhang, *Biophys. J.*, 2005, **88**, 4262–4273.